

Cyber Attacks Detection, Prevention, and Source Localization in Digital Substation Communication using Hybrid Statistical-Deep Learning

Nicola Cibir, Bas Mulder, Herman Carstens, Peter Palensky, Alexandru Ștefanov

Abstract—The digital transformation of power systems is accelerating the adoption of IEC 61850 standard. However, its communication protocols, including Sampled Values (SV), lack built-in security features such as authentication and encryption, making them vulnerable to malicious packet injection. Such cyber attacks can delay fault clearance or trigger unintended circuit breaker operations. While most existing research focuses on detecting cyber attacks in digital substations, intrusion prevention systems have been disregarded because of the risk of potential communication network disruptions. This paper proposes a novel method using hybrid statistical-deep learning for the detection, prevention, and source localization of IEC 61850 SV injection attacks. The method uses exponentially modified Gaussian distributions to model communication network latency and long short-term memory and Elman recurrent neural network to detect anomalous variations in the estimated probability distributions. It effectively discards malicious SV frames with minimal processing overhead and latency, maintains robustness against communication network latency variation and time-synchronization issues, and guarantees a near-zero false positive rate in non-attack scenarios. Comprehensive validation is conducted on three testbeds involving industrial-grade devices, hardware-in-the-loop simulations, virtualized intelligent electronic devices and merging units, and high-fidelity emulated communication networks. Results demonstrate the method’s suitability for practical deployment in IEC 61850-compliant digital substations.

Index Terms—Cyber Attacks, Deep Learning, Digital Substations, IEC 61850 Sampled Values, Intrusion Detection and Prevention System, Statistical Analysis.

I. INTRODUCTION

As proved by the latest cyber attacks on Ukraine’s power grid in 2015, 2016, and 2022 [1]–[3], and the attempted one on the United Kingdom’s power grid in 2020 [4], it is crucial to provide Industrial Control Systems (ICS), and, in broader terms, Operational Technology (OT) infrastructures, with state of the art cyber security controls to ensure a secure and resilient power system operation. The growing integration of Information Technology (IT) and OT infrastructures enables

efficient power system operation and management. However, it also expands the attack surface and increases the risk of cyber attacks by introducing new cyber security threats [5].

Communication protocols such as those defined in IEC 61850 standard have been developed for advanced protection, automation and control in digital substations. IEC 61850 notably lacks fundamental network security features such as authentication and encryption. This deficiency is especially evident in the IEC 61850 Sampled Values (SV) protocol, where the absence of robust security mechanisms allows malicious actors to inject crafted packets into the substation OT communication network, potentially leading to major disruptions such as delayed fault clearance or unintended circuit breaker operations. Furthermore, these OT disruptions can affect power system stability, cause cascading failures and lead to power outages or even a complete blackout [6], [7].

A viable option for defending against cyber attacks on digital substations is the deployment of network and host-based Intrusion Detection and Prevention Systems (IDS and IPS, respectively). Whereas a plethora of different IDSs for smart grids have been proposed in the literature [8], the deployment of IPSs in digital substations has been disregarded due to the general reluctance to implement such solutions in OT infrastructures. This reluctance arises from the risk of potential OT communication network disruptions, increased communication latencies, packet drops, and required computational resources. In this paper, a novel method is proposed for the detection, prevention, and source localization of IEC 61850 SV-based cyber attacks on digital substations.

The contributions of this paper are summarized as follows:

- 1) We present the first integrated system for intrusion detection, prevention, and attack source localization to protect against IEC 61850 SV injection attacks in digital substations. The method leverages statistical features of SV frames arrival times. The Exponentially Modified Gaussian (EMG) distribution is used to accurately model OT communication network latency variations and devices clock drift during time synchronization loss holdover conditions.
- 2) We propose a real-time hybrid method that combines statistical modeling with Deep Learning (DL) to identify and mitigate all known types of SV injection attacks. The proposed method ensures a near-zero False Positive Rate (FPR) when no cyber attacks are conducted, introduces negligible additional communication latency, and provides a throughput of more than 100,000 SV frames

This work was supported in part by the EU Horizon 2020 Marie Skłodowska Curie InnoCyPES Project with Grant Agreement No. 956433, and in part by the EU Horizon Europe ESTELAR Project with Grant Agreement No. 101192574. (Corresponding author: Alexandru Ștefanov)

Nicola Cibir, Peter Palensky, and Alexandru Ștefanov are with the Department of Electrical Sustainable Energy (ESE), Delft University of Technology, Mekelweg 4, 2628CD, Delft, The Netherlands (e-mails: {n.cibir, p.palensky, a.i.stefanov}@tudelft.nl).

Bas Mulder is with DNV Netherlands B.V., Utrechtseweg 310, 6812AR Arnhem, The Netherlands (e-mail: bas.mulder@dnv.com).

Herman Carstens is with Elia Group Innovation, Keizerslaan 20, 1000 Brussel, Belgium (e-mail: herman.carstens@elia.be).

per second. This makes the proposed method suitable for deployment in digital substations. Furthermore, the proposed method is resilient to communication network latency variations and time-synchronization issues among devices.

- 3) We extend the core method to detect and localize the compromised Intelligent Electronic Devices (IEDs) within High-availability Seamless Redundancy (HSR) rings. This is achieved by analyzing the spatial-temporal correlations in the Probability Distribution Functions (PDFs) of the SV frames arrival times across multiple IEDs.

The proposed method is validated and evaluated on three IEC 61850-compliant testbeds including industrial-grade devices, i.e., network switches, IEDs, Merging Units (MU), Hardware-in-the-Loop (HIL) simulations, virtualized IEDs (vIEDs), virtualized MU (vMU), and high-fidelity emulated substation OT communication network and components.

The remainder of the paper is organized as follows. In Section II, background information about the SV protocol and its cyber security concerns are provided. In Section III, state-of-the-art solutions for the detection and prevention of SV injection attacks are discussed and compared with the method proposed in this work. The proposed method is described in Section IV and then extensively validated and evaluated in Section V. Finally, Section VI concludes the paper.

II. BACKGROUND

A. IEC 61850 Sampled Values

IEC 61850 SV is a publisher-subscriber protocol used for three-phase current and voltage measurements reporting from MUs to IEDs. MUs publish SV frames in multicast, whereas IEDs process only the SV streams to which they are subscribed. The protocol was initially introduced in IEC 61850-9-2, further refined in IEC 61850-9-2LE, and ultimately standardized in IEC 61869-9. Various SV frame publishing rates are specified based on system frequency and application requirements. In digital substations, the most used rates are 4000 and 4800 frames per second for 50 Hz and 60 Hz power systems, respectively. Additionally, the standard defines the structure of SV frames, including the `smpCnt` field, a counter that increments with each published frame and resets to zero every second. Consequently, the `smpCnt` value ranges from zero to the number of frames published each second minus one. This part of the standard provides a certain level of determinism on the specific arrival time of each of the SV frames marked with a specific `smpCnt` value. In fact, given a specific second i , a predefined number of frames per second FS , and a `smpCnt` field value c , the theoretical frame arrival time $F_a^e(i, c)$ is computed as follows:

$$F_a^e(i, c) = i + c \cdot \frac{1}{FS}, \quad \forall c \in \{0, 1, \dots, FS - 1\} \quad (1)$$

As it will be discussed in Section IV, the determinism in the frames' arrival time gives an information advantage to discern legitimate and malicious SV frames, detect MitM attacks, and locate compromised IEDs within the OT communication network. To further increase the determinism of the SV frames

arrival time, as recommend in IEC 61850-90-4, priority tags and proper communication network engineering should be used to ensure the lowest possible latency for SV frames [9].

B. Sampled Values Cyber Security

Considering the strict latency requirements of power system protection schemes of 3 ms, the IEC 62351 standard stipulates against the application of digital signatures due to increased latency and processing times. To counteract most of the possible cyber attacks exploiting the SV protocol, the standard recommends the usage of Message Authentication Codes (MAC) relying on HMAC or AES-GMAC to provide message authentication. While appending the computed MAC to published frames helps mitigate replay and spoofing attacks, it also introduces multiple challenges and limitations. These include the increased device computational load, communication latency, and message overhead, need for Public Key Infrastructure (PKI) and Key Distribution Center (KDC) deployment, lack of support for legacy devices not supporting IEC 62351-6, and risk of pre-shared keys violation. Moreover, each device belonging to the same Group Domain of Interpretation (GDOI) has access to the same shared secret key, and thus can perform spoofing attacks.

Summarizing, once an attacker is able to gain access to the digital substation OT communication network [5], the cyber attacks that can be launched against an SV subscriber include: (1) flooding, where a large number of SV frames are injected into the communication network by the attacker to exhaust subscriber resources; (2) spoofing, where the attacker injects malicious SV frames pretending of being the legitimate SV publisher; (3) replay, where the attacker re-injects into the network previously sniffed SV frames; (4) high `smpCnt` attack, in which an attacker injects an SV frame with a high `smpCnt` field value, causing the SV subscriber implementing the replay protection mechanism as mandated in IEC 62351-6 to discard any further legitimate SV frame with a lower `smpCnt`; (5) Man-in-the-Middle (MitM), where an attacker takes control of a device forwarding SV frames from the publisher to the subscriber and tamper with the forwarded SV frames; (6) access to the pre-shared secret key, in which the attacker gains access to the pre-shared secret key used for MAC generation and validation.

In this paper, to evaluate the effectiveness of the proposed method, the performed cyber attacks assume the injection of malicious SV frames which are completely indistinguishable from the legitimate ones. In other words, the Hamming distance between the content of legitimate and malicious SV frames is equal to zero. By proving the method effectiveness in this worst-case scenario, the results can be extended to cases where false measurements are injected, thus leading to a Hamming distance greater than 0.

III. RELATED WORK

To address the security concerns presented in the previous sections, several works proposed and evaluated the adoption of authentication and/or encryption for GOOSE and SV [10]–[14]. However, the usage of cryptographic schemes raises

challenges and limitations as discussed in Section II. Other works proposed novel methodologies for intrusion detection considering the measurements reported in the SV frames. In [15], several Machine Learning (ML) algorithms are tested to detect False Data Injection (FDI) attacks by analyzing the measurements contained in the SV frames and distinguishing between normal and abnormal micro-grid and substation behaviors. Even the most promising solution, which relies on extreme randomized trees, provides good but not impressive performances, with an F1-score of around 91% depending on the different FDI attacks and fault combinations.

In [16], an algorithm based on immune system of negative selection and self-shape optimization is introduced to distinguish between busbar faults and SV attacks. The proposed detector focuses on assessing the validity of the measurements received and provides promising detection performance with a True Positive Rate (TPR) and FPR of around 93% and 7%, respectively, but causes an operation delay ranging from 0.48 to 9.21 ms. Another approach is described in [17], where a neural network-based forecaster is used to detect spoofed SV frames. Whenever a replay attack is detected by checking the `smpCnt` field value, the frame is sent to the anomaly detector which, using the latest 20 measurements received through the SV stream, estimates the next expected measurement, and if the difference between the forecasted measurement value and the received one is above a certain threshold, the frame is marked as malicious and discarded. A key limitation of this type of IDS is that relying on reported measurements can be misleading during replay attacks where normal operating conditions are injected. In such cases, the measurements appear consistent with the physical model used for validation. To overcome this limitation, other authors proposed IDSs considering network traffic and SV frames information. These solutions rely on information such as the number of SV frames received each second (FS), the received frames' `smpCnt`, the Inter-Frame Arrival Time (I-FAT), and the frames' arrival time (F_a).

In [18], a solution to detect FDI attacks on GOOSE and SV is presented. For what concerns the SV stream injection part, the proposed solution checks that the `smpCnt` field of the received SV frames is always increasing. The time required to perform the replay attack protection is equal to 0.013 ms, which is below the inter-frame arrival delay of 0.21 ms, and comparable to the processing times of other solutions (0.006, 0.29, 0.049 ms for the solutions proposed in [13], [17], and [15], respectively). However, this type of solution is not enough to detect advanced SV injection attacks, e.g., MitM. In [19], a feed-forward neural network is used to correlate two SV stream parameters, i.e., FS and I-FAT, with the SV publisher that published the SV stream in the network. The proposed method achieves high accuracy in identifying the source publisher of a received stream. However, this performance is attributed to the fact that the second publisher did not attempt to replicate the identity of the first. If impersonation was attempted, a malicious publisher could emulate the SV stream parameters used by the classifier, potentially bypassing detection.

In [20] and [21], a network-based Anomaly Detection

TABLE I
COMPARISON OF THE DISCUSSED SOLUTIONS IN TERMS OF INFORMATION USED FOR ATTACK DETECTION. (Y=YES, N=NO, P=PARTIAL).

	PHY	FS	smpCnt	I-FAT	F_a
Ustun et al. [15]	Y	N	N	N	N
Mo et al. [16]	Y	N	N	N	N
El Hariri et al. [17]	Y	N	Y	N	N
Hussain et al. [18]	Y	N	Y	N	N
Wannous et al. [19]	N	Y	N	Y	N
Hong et al. [20], [21]	N	Y	Y	N	N
Eynawi et al. [22]	Y	N	N	Y	Y
Delhomme et al. [23]	N	N	Y	Y	Y
Manzoor et al. [24]	Y	N	Y	N	Y
Hong et al. [25]	N	Y	Y	N	N
Our Solution	N	Y	Y	Y	Y

TABLE II
DISCUSSED SOLUTIONS' PROTECTION CAPABILITY AGAINST DIFFERENT TYPES OF ATTACKS. (Y = YES, N = NO, P = PARTIAL).

	(1)	(2)	(3)	(4)	(5)	(6)
Ustun et al. [15]	N	Y	N	N	P	Y
Mo et al. [16]	N	Y	N	N	P	Y
El Hariri et al. [17]	N	N	Y	Y	P	Y
Hussain et al. [18]	P	N	Y	N	N	Y
Wannous et al. [19]	N	N	N	N	N	Y
Hong et al. [20], [21]	P	N	Y	N	N	Y
Eynawi et al. [22]	N	N	Y	N	N	Y
Delhomme et al. [23]	P	N	N	N	N	Y
Manzoor et al. [24]	N	N	Y	Y	N	Y
Hong et al. [25]	P	N	Y	Y	N	Y
Our Solution	P	Y	Y	Y	Y	Y

System (ADS) to detect malicious activities of GOOSE and SV across substations is presented and then further expanded. For what concerns SV, the system relies on three violation control methods to detect the anomalies. The first violation method checks the number of SV frames received in the last second, and if this value is higher than the threshold value, the anomaly is identified. The second method offers replay protection by checking that the `smpCnt` field value is always increasing. Finally, the last check verifies that the SV stream identifier and name did not change, implying that the MU configuration did not change. When one of these three methods detects an anomaly, an alert is sent to the operator and a disconnect control command is sent to the firewall to block the intruder's connection. Even though the performed simulation results confirm excellent detection performance, with FPR and False Negative Rates (FNR) equal to 0.013% and 0.02%, respectively, it is unclear how the firewall can block intruder's SV injected stream, but not the original one, given that it is not possible to discern the original and injected SV frames. This is of crucial importance, otherwise for the attacker it would be enough to send one single SV frame to the ADS to block the original SV stream reception. Also, if an attacker can block the original SV stream and inject its own, the proposed ADS wouldn't be able to detect the attack because the number of SV frames received by the IED will not be more than the set threshold, the counter of the injected frames can be easily set by the attacker as always increasing, and the stream identifier can be matched with the one of the original SV stream published by the legitimate MU.

In [25], a collaborative intrusion detection and prevention

system for GOOSE and SV is presented. For SV, the number of received SV frames and the consistency of the `smcCnt` parameter are checked. When an anomaly is detected, the protection scheme is disabled to prevent unintended circuit breaker operations and thus leading to an implicit Denial of Service (DoS) caused by the IPS. In [22], a ML-based feature selection algorithm for detecting attacks targeting MMS and SV protocols is proposed. After feature selection, the tested Random Forest (RF)-based IDS provides an accuracy of 99.91% in detecting standard SV injection attacks. Still, the methodology fails in detecting more advanced attacks, e.g., replay with spoofing or MitM. In [23], different ML models for the detection of DoS attacks are presented; still, even the most effective model, that is RF, provides an accuracy of 84.12%. Finally, in [24], an approach leveraging the in-context learning ability of transformer architecture for the detection of novel attacks against IEC 61850 protocols is introduced. The proposed methodology reaches an accuracy close to 100% for the detection of SV injection and replay attacks, but results are not provided for the detection of advanced attacks, e.g., spoofing and MitM. Moreover, the time required for detecting the attacks ranges from 2,44 to 100 ms depending on the available computation power. This does not allow the methodology to be applied for real-time intrusion prevention purposes.

In Tables I and II, the solutions proposed in the literature are compared in terms of information used for intrusion detection, and protection capabilities against the attacks described in Section II. It is worth mentioning that, contrary to our solution, none of the solutions proposed in the literature can identify the source of the SV attack and allow the protection scheme to operate without any additional negligible delays during a cyber attack.

IV. CYBER ATTACKS DETECTION, PREVENTION, AND SOURCE LOCALIZATION

Fig. 1 represents the architecture of the proposed method. It can be divided into two main modules, i.e., (1) intrusion detection and prevention module, which is deployed in each IED, and (2) attack source localization module, which is deployed on a centralized location within the digital substation and receives statistical information from each IED. In the following, theoretical preliminaries and the different components and their interactions are presented.

A. SV Frames Arrival Time Shift

As introduced in Section II, the IEC 61869-9 standard mandates strict timing specifications for SV publishers. Given that in real communication networks, the theoretical frame arrival time is affected by frame transmission, propagation, queuing, and processing delays, and time synchronization errors among SV stream publisher and subscriber devices, each frame is received at a time $F_a^{real}(c) \neq F_a^e(c)$, within each second. By monitoring the SV subscriber Network Interface Card (NIC), for each received frame it is possible to measure

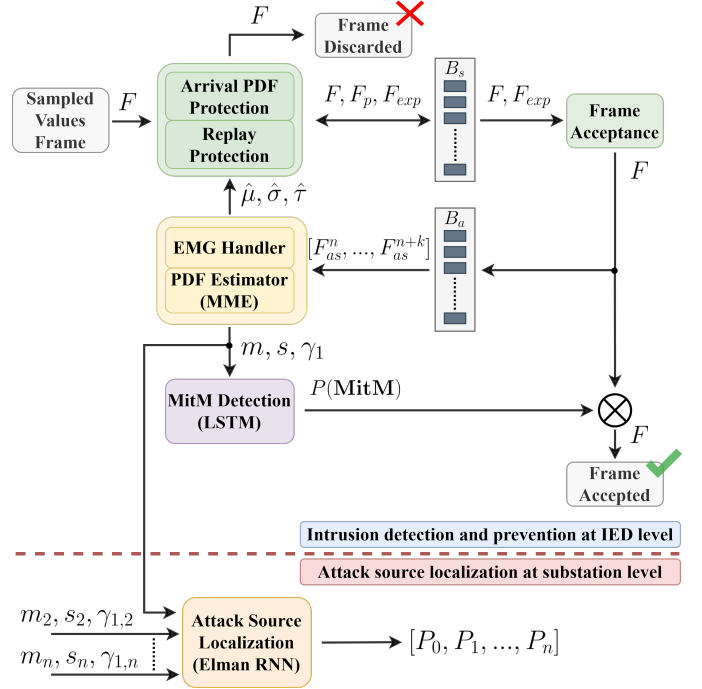


Fig. 1. Hybrid statistical-deep learning-based intrusion detection, prevention, and attack source localization system architecture.

$F_a^{real}(c)$, and consequently, compute the difference between the theoretical and empirical frame arrival time as in (2).

$$F_{as} = F_a^{real}(c) - F_a^e(c), \quad \forall c \in \{0, 1, \dots, FS - 1\} \quad (2)$$

To account for the stochasticity of the communication network infrastructure, a PDF can be estimated over F_{as} . Then, the modeled PDF can be used as an information advantage for intrusion detection, prevention, and attack source localization. Indeed, once that this PDF is estimated, it allows to assign a probability for each frame of being legitimate, thus allowing to discern legitimate and malicious SV frames depending on their F_{as} measured at the subscriber. Regarding the choosing of the appropriate PDF to be used, it has been shown in the literature that latency in communication networks can be modeled as an Exponential distribution [26]. Unfortunately, the Exponential distribution assigns a probability equal to zero for any sample lower than the lower bound of its support and thus limits the modeling capabilities of scenarios in which a reduction of communication latency is measured due to devices time synchronization errors. To overcome these challenges, an EMG distribution is used to model F_{as} .

B. Exponentially Modified Gaussian Distribution

The EMG distribution is a probability distribution that results from the convolution of a normal distribution, $Z \sim \mathcal{N}(\mu, \sigma^2)$, with an exponential one, $E \sim \text{Exp}(\lambda)$. An EMG distribution is characterized by the following PDF:

$$f(x) = \frac{\lambda}{2} e^{\frac{\lambda}{2}(2\mu + \lambda\sigma^2 - 2x)} \text{erfc}\left(\frac{\mu + \lambda\sigma^2 - x}{\sqrt{2}\sigma}\right) \quad (3)$$

where μ and σ are the mean and standard deviation of the normal distribution, respectively, and $\lambda = 1/\tau$ is the

exponential decay of the Exponential distribution. Due to the changing operating conditions, F_{as} can vary in time, and thus EMG distribution parameters need to be continuously estimated and updated using the latest received SV frames. As proven by Ali et al. [27], the Method of Moments Estimation (MME) provides the best trade-off in terms of parameters estimation accuracy and efficiency. In fact, to minimize SV frames classification latency, an accurate estimator providing a closed form solution is required. By using the MME, it is possible to equate the first three theoretical moments of the EMG distribution with the three empirical ones as in (4), (5), and (6), for the mean (m), variance (s^2), and skewness (γ_1), respectively:

$$\mathbb{E}[X] = m = \mu + \tau = \hat{m}_1 \quad (4)$$

$$\text{Var}(X) = s^2 = \sigma^2 + \tau^2 = \hat{m}_2 \quad (5)$$

$$\gamma_1 = \frac{2\tau^3}{(\sigma^2 + \tau^2)^{3/2}} = \frac{\hat{m}_3}{\hat{m}_2^{3/2}} \quad (6)$$

where \hat{m}_r is the r -th empirical moment computed on the observed data. As shown in Oliver et al. [28], solving for the EMG distribution parameters gives:

$$\hat{\mu} = m - s \left(\frac{\gamma_1}{2} \right)^{1/3} \quad (7)$$

$$\hat{\sigma}^2 = s^2 \left[1 - \left(\frac{\gamma_1}{2} \right)^{2/3} \right] \quad (8)$$

$$\hat{\tau} = \frac{1}{\lambda} = s \left(\frac{\gamma_1}{2} \right)^{1/3} \quad (9)$$

where $\hat{\mu}$, $\hat{\sigma}$, and $\hat{\lambda}$ are the estimated PDF parameters.

C. Intrusion Detection and Prevention

To discern legitimate and malicious SV frames on a per frame basis in real-time, and to detect advanced MitM attacks, the proposed method relies on four interdependent components being executed in parallel in each IED. Moreover, two buffers, i.e., the Staging Buffer (B_s) and Accepted Frames Buffer (B_a), are used to store the latest received frames which are most likely to be legitimate and the last k accepted frames, respectively.

1) *Arrival PDF and Replay Protections*: Once a new SV frame is received at the subscriber NIC, it is processed by the first component. First, it is checked whether frames with the same `smPCnt` value were already accepted in the current time period. If it is the case, the replay protection mechanism is triggered, and the frame is discarded. Then, after computing F_{as} for the current frame as presented in the previous section, the EMG PDF (ϕ_{EMG}) is used to compute the probability of the frame being legitimate (F_p), such that $F_p = \phi_{EMG}(F_{as})$. Subsequently, the component checks whether in B_s a frame with the same `smPCnt` value as the just received frame is present. If such a frame is already present, but the probability of it being legitimate is higher than the one computed on the last received frame, the last received frame is discarded. Otherwise, if no frame with the same `smPCnt` is present in B_s , or the legitimacy likelihood of the new frame is higher, the

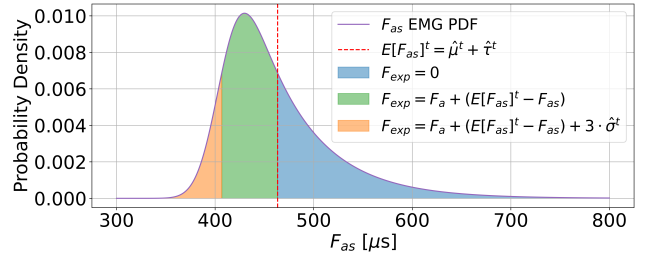


Fig. 2. Graphical interpretation of F_{exp} value assignment.

just received frame is inserted in the buffer, and the already present one is discarded. In this way, it is guaranteed that exactly FS frames per second are accepted and no false positive can occur when no cyber attack is ongoing. Other than computing F_p , a frame expiration time (F_{exp}) is assigned to each frame added to B_s , with F_{exp} computed as follows:

$$F_{exp} = \begin{cases} 0, & F_{as} \geq \mathbb{E}[F_{as}]^t \\ F_a + r, & F_p \geq \varphi_{EMG}(\mathbb{E}[F_{as}]^t) \\ F_a + r + 3 \cdot \hat{\sigma}^t, & \text{otherwise} \end{cases} \quad (10)$$

where the residual r is equal to $\mathbb{E}[F_{as}]^t - F_{as}$.

The rationale behind the values assigned to F_{exp} is to minimize the time spent by the frames in B_s while guaranteeing the acceptance of the SV frames with the highest likelihood of being from the legitimate device and not from the attacker. In fact, if a frame with `smPCnt` equal to c is received at time F'_a , and the computed F'_{as} is equal to or greater than $\hat{\mu}^t + \hat{\tau}^t = \mathbb{E}[F_{as}]^t$, then, for any other frame with the same `smPCnt` received at a time $F''_{as} > F'_{as}$, $\varphi_{EMG}(F''_{as}) = F''_p$ will be lower than $\varphi_{EMG}(F'_{as}) = F'_p$. Thus, the frame can be accepted immediately without any further delay. In the other cases, it cannot be guaranteed that in the future frames with higher legitimacy likelihood will not be received, and thus the received frame needs to be retained until F_{exp} . A graphical interpretation on the values assigned to F_{exp} is provided in Fig. 2. Moreover, the pseudocode for this component is provided in Algorithm 1.

2) *Frame Acceptance*: This component is responsible for processing SV frames stored in B_s , while continuously monitoring whether the current time is higher than frames' F_{exp} . If this condition holds, it implies that no additional SV frames with higher likelihood of legitimacy are expected to be received. Thus, the SV frame currently stored in B_s can be accepted, forwarded to the protection scheme for immediate use, and added to B_a , which stores the SV frames used for updating the parameters of the EMG PDF.

3) *EMG Handler and PDF Estimator*: After the number of SV frames in B_a is greater than k , this component takes care of estimating and updating the parameters of the EMG distribution. This is done by first updating the samples' moments with a weighted mean between the previously calculated moments (\hat{m}_r^t) and the just computed ones (\hat{m}_r), as in (11), and then using the updated moments values to compute the updated EMG parameters $\hat{\mu}^{(t+1)}$, $\hat{\sigma}^{(t+1)}$, and $\hat{\lambda}^{(t+1)}$.

$$\hat{m}_r^{(t+1)} = \frac{FS \cdot \hat{m}_r^t + k \cdot \hat{m}_r}{FS + k} \quad (11)$$

Algorithm 1 SV frame likelihood (F_p) and expiration (F_{exp}) computation, and push frame to staging buffer.

Inputs: SV frame (F)
Variables: Variables: B_s , F_a , F_p , F_{exp} , frame `smpCnt` field value (F_{smpCnt}), function returning EMG PDF value at x ($\varphi_{EMG}(x)$), EMG expected value ($\mathbb{E}[F_a^t]$), EMG standard deviation ($\hat{\sigma}^t$).

```

ARRIVAL_PDF_AND_REPLAY_PROTECTIONS( $F$ ):
  if  $|F_{as} - \mathbb{E}[F_{as}]^t| \geq 5 \cdot \hat{\sigma}^t$ 
    discard  $F$  # flooding attack mitigation
    return
   $F_p \leftarrow \varphi_{EMG}(F_{as})$ 
  if  $F_{as} \geq \mathbb{E}[F_{as}]^t$ 
     $F_{exp} \leftarrow 0$ 
  else if  $F_p \geq \varphi_{EMG}(\mathbb{E}[F_{as}]^t)$ 
     $F_{exp} \leftarrow F_a + (\mathbb{E}[F_{as}]^t - F_{as})$ 
  else
     $F_{exp} \leftarrow F_a + (\mathbb{E}[F_{as}]^t - F_{as}) + 3 \cdot \hat{\sigma}^t$ 
   $B_s^{len} \leftarrow \text{length}(B_s)$ 
  if  $B_s^{len} == 0$  or  $B_s[B_s^{len}]_{F_{smpCnt}} < F_{smpCnt}$ 
     $B_s[B_s^{len}] \leftarrow [F, F_p, F_{exp}]$ 
    return
  for  $j \leftarrow 0, \dots, B_s^{len}$ 
    if  $B_s[j]_{F_{smpCnt}} > F_{smpCnt}$ 
       $B_s[j] \leftarrow [F, F_p, F_{exp}]$ 
      return
    if  $B_s[j]_{F_{smpCnt}} == F_{smpCnt}$ 
      if  $B_s[j]_{F_p} < F_p$ 
         $B_s[j] \leftarrow [F, F_p, F_{exp}]$ 
    else
      discard  $F$ 
  return

```

The updated EMG parameters are then used by the arrival PDF and replay protections component to evaluate the legitimacy of any SV frame that arrived subsequently.

4) *MitM Detection*: Whereas the first component is meant to accept exactly FS SV frames per second while reducing the likelihood of malicious frames being accepted, this third component aims at detecting advanced MitM attacks. In this type of attack, it is assumed that the attacker can completely block the legitimate SV stream and inject a malicious one. Thus, the subscriber device receives exactly FS frames per second as expected. Still, the act of intercepting and tampering with the forwarded SV frames causes an inevitable change in the statistics of the received SV stream at the subscriber level. In fact, to perform the MitM attack, the attacker is required to change the NIC configuration of the compromised forwarding device to disable the HSR bridge between the two NICs. Then, the network traffic needs to be monitored, tampered with, and forwarded from one NIC to the other at the device application layer, causing the inevitable alteration of the forwarded traffic statistical properties. To detect these changes, a Recurrent Neural Network (RNN) is deployed to detect anomalous variations in the EMG parameters. The input of the RNN consists of the mean (m), standard deviation

(s), and skewness (γ_1) of the F_{as} measured on the accepted frames, calculated over a sliding window of 200 samples with a step size of 50 samples. The RNN outputs the likelihood of an ongoing MitM attack. A grid search approach is used to select the most appropriate RNN model and perform hyperparameter optimization. The considered RNN models include Elman RNN, Long-Short Term Memory (LSTM), and Gated Recurrent Units (GRU), whereas the dimension and the number of hidden layers vary from 3 to 20 and from 2 to 8, respectively. The model providing the best trade-off between model complexity, detection accuracy, and prediction time consists of 4 stacked LSTM cells of 20 neurons each. Finally, to perform the binary classification, a fully connected layer is stacked to the output of the last LSTM cell.

D. Attack Source Localization

As mentioned in the previous section, anomalous changes in the PDF of F_{as} can be an indicator of an ongoing MitM attack. By aggregating and correlating the statistical properties of the SV frames arrival times from different IEDs deployed within the digital substation it is possible to identify and locate which device is performing a MitM attack. In this paper, the focus is on IEDs deployed in a HSR ring topology. As represented in Fig. 1, the mean (m_i), standard deviation (s_i), and skewness ($\gamma_{(1,i)}$) of the measured F_{as} from each i -th IED are delivered to the server hosting the attack source localization module within the digital substation. These metrics are then used to estimate the probability of a MitM attack being ongoing, and the probability for each IED of acting maliciously. As for the MitM component, a sliding window of 200 F_{as} samples with a step size of 50 samples is used. This last component consists of 5 stacked Elman RNN cells; each cell hidden layer contains 26 neurons. The tanh activation function is used. The output of the last RNN cell is provided as input to a fully connected layer to perform the final multi-class classification. To improve the DL model accuracy and increase its generalization capabilities, the component's input data is derived from the statistical metrics received from each IED as follows:

$$\forall t \in \{1, \dots, T\}, i, j \in \{1, \dots, N\}, i < j:$$

$$\begin{cases} m_{(i,j)}^t = m_i^t - m_j^t \\ s_{(i,j)}^t = s_i^t - s_j^t \\ \gamma_{(1,i,j)}^t = \gamma_{(1,i)}^t - \gamma_{(1,j)}^t \end{cases} \quad (12)$$

where t is the current time window, N is the number of IEDs deployed in the HSR ring, and m_n^t , s_n^t , and $\gamma_{(1,n)}^t$ are the mean, standard deviation, and skewness measured at n -th IED at time t . This data transformation prevents the DL model from overfitting the absolute values measured in the specific communication network conditions, but to focus more on the relative evolution of the statistical properties.

E. Attacker Considerations

From an attacker's perspective, to deceive the proposed method several non-trivial challenges need to be overcome. First, estimating F_{as} for a specific SV subscriber from a

different device requires the estimation of the overall communication latency between the legitimate publisher and the targeted subscriber, and between the compromised device and the targeted subscriber. Furthermore, this estimation needs to keep into account also the timing synchronization errors. Second, to inject the SV frames at the exact time instant required to match the expected F_{as} , the compromised device needs to be executing a real-time operating system and be time synchronized with Precision Time Protocol (PTP). Moreover, to carry out the attack, a malicious script capable of publishing SV frames must be delivered and deployed on the compromised device. This deployment must occur stealthily, avoiding detection by both host-based and network-based IDSs; also, the script execution should not exhaust compromised device resources. Finally, to cause protection schemes to react to a fault, it is not sufficient to have only a small number of false measurements to be accepted. For instance, when overcurrent protection is implemented, the measured current needs to be above a certain threshold for at least 200 ms. This means that an attacker needs at least $FS/5$ consecutive malicious frames to be accepted to trigger the protection scheme. Thus, the injected malicious frames need to be consistently accepted for a non-negligible amount of time. All these required conditions combined make it extremely difficult for an attacker to successfully deceive the proposed method even in ideal conditions.

V. EXPERIMENTAL RESULTS AND DISCUSSION

The proposed method was extensively tested on data acquired from three different IEC 61850-compliant testbeds. The first testbed consists of Real-Time Digital Simulator (RTDS) simulating an IEEE 5-bus system, a GTNETx2 card acting as SV publisher, a network switch, and three vIEDs connected in an HIL configuration and acting as SV subscribers. The second testbed is deployed by Elia transmission system operator in Belgium and consists of industrial-grade devices deployed in a Parallel Redundancy Protocol (PRP) configuration. In this second case, the deployed devices include an MU publishing an SV stream, two network switches, and an IED. Finally, the third testbed consists of a fully virtualized setup in which the digital substation communication network was emulated in Mininet. The setup consists of two HSR rings corresponding to the process and station buses, connected through a QuadBox, and containing 4 vMUs and 5 vIEDs, respectively. In the first two testbeds, the tests consisted in the execution of SV injection attacks from a compromised device connected to the network switch taking care of forwarding SV streams from the publisher to the subscriber. The injected false measurements represented an ongoing fault which successfully caused the (v)IEDs to react and issue an unintended command to open a circuit breaker.

The objective of the IPS was to prevent the malicious SV frames from being processed by the protection scheme while minimizing the number of legitimate frames being dropped. It should be noted that the IPS did not rely on the measurements content for frames classification, thus the difference between the legitimate and malicious measurements was not relevant

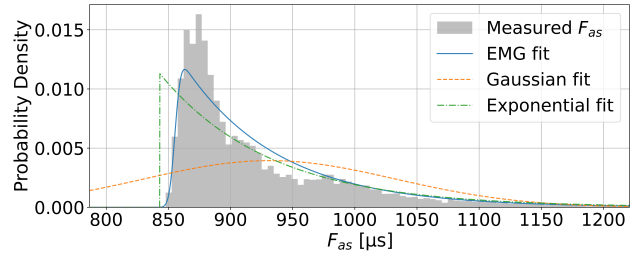


Fig. 3. Demonstration of EMG distribution fitting capabilities.

for this performance evaluation and can be assumed to be zero. On the other hand, the third testbed was used to monitor network traffic during MitM attacks; this data was then used for the training and testing of the attack source localization module. To acquire the data needed for the validation of the proposed method, Wireshark was run on each (v)IED belonging to the three testbeds. Fig. 3 shows how EMG distribution fits the measured F_{as} values at one vIED deployed in the third testbed. As can be seen, the EMG distribution provides better fitting capabilities compared to Exponential and Gaussian distributions.

In Table III, the main information about the monitored SV streams in the first two testbeds during normal conditions is reported. This information includes the number of frames received per second (FS), measured F_{as} mean and standard deviation, and the overall time synchronization error due to the lack of time synchronization with the PTP master clock. It should be noted that to comply with IEC 61850-9-3, each IED should guarantee a maximum holdover of $\pm 0.2 \mu s/s$, thus implying a maximum time synchronization divergence among two devices of $\pm 0.4 \mu s/s$. Given the holdovers experienced during our tests, it is fair to claim that the proposed method was tested in the most critical conditions that could be found in a real digital substation scenario. In the following, each component performance is evaluated in detail.

A. Intrusion Prevention Evaluation

To effectively evaluate the performance of the proposed intrusion prevention method, the TPR, FPR, and F1-score metrics are considered. In fact, for a fair evaluation it is crucial to keep into consideration and maximize the TPR while minimizing the FPR. This is because a considerable number of consecutive false negatives could lead the (v)IED to issue unintended control commands to circuit breakers. Conversely, if many legitimate SV frames are discarded because they are wrongly classified, the protection algorithm is

TABLE III
INFORMATION ABOUT THE MONITORED SV STREAMS AT DIFFERENT (v)IEDs.

	vIED ₁	vIED ₂	vIED ₃	IED ₁
FS [frames/s]	4800	4800	4800	4000
$\mathbb{E}[F_{as}]$ [ms]	-7.08	-4.60	0.447	-113.30
F_{as} std. dev [μs]	53	123	104	25
Holdover [μs]	-1.399	1.658	-0.032	-0.371

TABLE IV
IPS PERFORMANCES AGAINST SV INJECTION ATTACKS PERFORMED ON
THE TWO TESTBEDS.

	vIED ₁	vIED ₂	vIED ₃	IED ₁
# Legitimate frames	43124	43124	43124	50000
# Malicious frames	19201	19201	19201	50000
$\mathbb{E}[F_{as}^{(mal-leg)}]$ [μs]	-178	-223	-205	1001
FPR [%]	0.67	0.42	0.77	0.005
TPR [%]	98.50	99.74	98.78	100
Precision [%]	98.49	99.07	98.28	100
F1-Score [%]	98.49	99.41	98.53	100

prevented from operating properly and timely. Before testing the IPS against SV injection attacks, its performances in terms of false positives during normal operating conditions are evaluated. During normal conditions, the IPS caused FPR of 0.07%, 0.35%, 0.32%, and 0.005% on vIED1, vIED2, vIED3, and IED1, respectively. These false positives were mainly caused by frames being received with an unexpected latency greater than 3 ms. Indeed, as can be noted in Table III, higher FPR resulted in (v)IEDs experiencing higher levels of communication jitter, i.e., higher variance of F_{as} . Given that the IEC 61850 standard mandates a maximum latency of 3 ms, these frames should have been discarded anyway by the protection scheme and thus should not be considered an actual misbehavior of the proposed IPS. Subsequently, malicious SV streams were injected into the network from a compromised machine connected to the network switch in the first and second testbeds. Due to the attacker's challenges discussed in Section IV, perfectly matching the expected F_{as} was not feasible. In fact, after several trials and adjustments, the minimum difference between the frame arrival time shift expected by the SV subscriber (F_{as}^{leg}) and frame arrival time shift of the frames injected by the attacker (F_{as}^{mal}) was of $-178 \mu s$. The difference between F_{as}^{leg} and F_{as}^{mal} , which will be referred to as $F_{as}^{(mal-leg)}$, can be seen as the attacker injection time shift error. As can be appreciated in Table IV, even with such small attacker injection time shift errors, the IPS provided FPRs lower than 0.77% and TPRs higher than 98.5%.

To accurately estimate the IPS performance in function of $F_{as}^{(mal-leg)}$, a synthetic dataset was generated starting from the original one. In the synthetic dataset, the original legitimate frames were duplicated, and then the duplicated frames F_{as} was varied such that the values of $F_{as}^{(mal-leg)}$ were included within $\pm 600 \mu s$. These duplicated frames represented the malicious frames injected by the attacker. As can be observed in Fig. 4, the IPS provided great prevention capabilities down to an attacker injection error of less than $\pm 100 \mu s$, with FPRs lower than 1% and F1-scores above 95%. Higher $F_{as}^{(mal-leg)}$ absolute values were not considered because they would lead to F1-scores close to 100%. As expected, the limitation of the proposed IPS comes into play when the attacker matches the expected legitimate F_{as} . In that case, the information advantage is lost, and legitimate and malicious frames have a 50% probability of being accepted or discarded. Final consideration regards the IPS added latency and throughput performances. Throughout the tests, it was verified that the IPS introduced an additional latency of less than $100 \mu s$ and

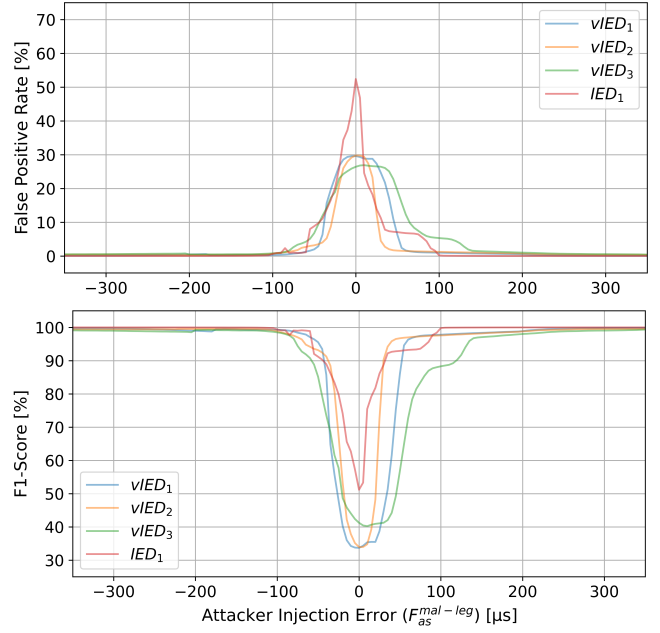


Fig. 4. Intrusion prevention method FPR and F1-score with varying attacker injection error ($F_{as}^{(mal-leg)}$) on the four (v)IEDs.

sustained a throughput exceeding 100,000 frames per second. These performances satisfy the stringent timing requirements specified in IEC 61850-5 and support the highest SV frames publishing rate of 96,000 frames per second, as defined in IEC 61869-9.

B. MitM Detection Evaluation

The MitM attacks detection component was evaluated on four synthetic datasets generated starting from the ones acquired from the first two testbeds. It was assumed that the attacker, by compromising a forwarding device and performing a MitM attack against the subscriber, could drop the legitimate SV stream and inject the malicious one. Thus, the SV subscriber received exactly the expected number of SV frames, i.e., FS , but, due to the MitM attack, the frames arrival time statistical properties were affected. This assumption was then validated on the fully virtualized setup, where the MitM attacks were practically performed. To generate the synthetic anomalous acquisitions, half of the legitimate data was modified by adding random variations in the measured F_{as} mean, standard deviation, and skewness. These random variations are referred to as Δm , Δs , and $\Delta \gamma_1$, with values drawn from Uniform distributions with lower and upper bounds of $\pm 300 \mu s$, $\pm 10\%$, and $\pm 5\%$, respectively. After selecting a detection threshold guaranteeing FPRs lower than 0.15% and 0.01% in the first and second testbeds, respectively, the MitM component provided TPRs of 95.15%, 95.99%, 93.85%, and 97.66%, for vIED1, vIED2, vIED3, and IED1, respectively. Still, it must be kept in consideration that in the generated synthetic dataset, some malicious samples were indistinguishable from the legitimate ones, due to random choosing of Δm , Δs , and $\Delta \gamma_1$ values close to zero. In Fig. 5, the evaluation results for the second testbed IED with varying Δm and Δs are depicted.

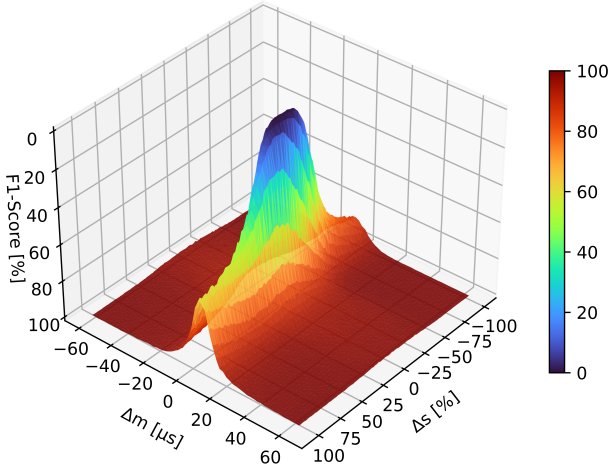


Fig. 5. F1-score of the MitM detection component in function of the alteration in F_{as} mean and variance due to the cyber attack.

Similar consideration can be drawn for the first testbed vIEDs. As can be appreciated, the MitM detection method provided an F1-score higher than 99.9% down to an Δm variation of 20 μs . This means that, to remain undetected, an attacker needs to alter the F_{as} measured by less than 20 μs on average. Moreover, even if a lower alteration is caused on the expected F_{as} mean, variations in the measured standard deviation or skewness of F_{as} still provide an information advantage to detect the ongoing MitM attack.

C. Attack Source Localization Evaluation

This last component was validated on network traffic acquired from the third testbed. To perform MitM attacks, each vIED in the HSR ring was compromised one at a time, its NICs' HSR bridge was disabled, and a C script was used to monitor, tamper, and forward SV frames. The network traffic was monitored with Wireshark at each vIED NIC. The network traffic was acquired during four different experimental scenarios. Each experimental scenario consisted of one case representing normal operating conditions and five cases with a MitM attack in place in one vIED, thus leading to 24 acquisitions in total to be used for the training and validation of the DL model. As for the validation of the MitM detection component, measured F_{as} mean, standard deviation, and

TABLE V
SEPARATION OF SCENARIOS AMONG TRAINING AND TESTING DATASET.

Scenario ID	1	2	3	4
Training set	normal anomalous	–	normal anomalous	normal
Testing set	–	normal anomalous	–	anomalous

TABLE VI
ATTACK SOURCE LOCALIZATION RESULTS ON THE TRAINING AND TESTING DATASETS.

	Accuracy	Precision	Recall	F1-score
Training set	99.810%	99.805%	99.807%	99.806%
Testing set	99.061%	99.096%	99.103%	99.099%

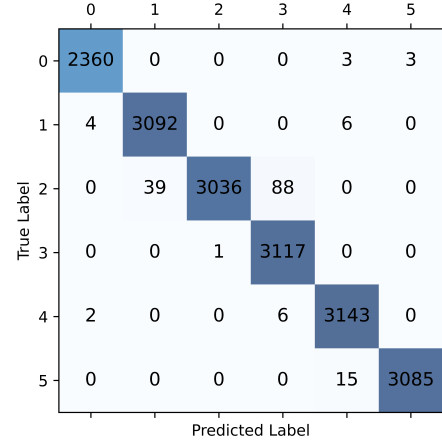


Fig. 6. Attack source localization confusion matrix on the testing set. Label "0" corresponds to normal conditions; labels from "1" to "5" denote which vIED is performing the MitM attack.

skewness were computed for each vIED, and then delivered to the attack source localization component. To further increase the realism of the experiments, the compromised vIED was allowed to report either normal or abnormal statistical metrics from both NICs. The DL model was trained on normal and anomalous cases of some experimental scenarios and then tested on normal and anomalous cases of other scenarios as reported in Table V; this allowed to further prove the generalization capabilities of the proposed DL-based method. In fact, in a real deployment scenario, only normal operating conditions can usually be acquired from the field and be used for training. However, as demonstrated in our experiments, the training set can be expanded with anomalous data acquired from an emulated network. The resulting trained model is then effective in detecting and localizing unseen MitM attacks in the real OT communication network. As reported in Table VI, both in the training and testing datasets, the attack source localization method provided accuracy, precision, recall, and F1-scores higher than 99%. Furthermore, as can be appreciated in Fig. 6, the number of false positives was limited to 6 out of 2366 normal operating conditions samples, resulting in a FPR of 0.25%. Also, when the source of the attack was mislocalized, most of the time the error was limited to devices adjacent to the malicious one. This limits the number of devices that require further investigation after a cyber security incident.

VI. CONCLUSIONS

This paper presents a novel hybrid statistical-deep learning-based method for the detection, prevention, and attack source location of IEC 61850 SV injection attacks in digital substations. It has been shown how the usage of SV frames arrival time statistics provides useful information to discern between legitimate and malicious SV frames, early detected advanced cyber attacks, e.g., MitM, and identify malicious IEDs within the digital substation communication network. As validated by the experimental results, the proposed method provides

promising intrusion detection and prevention performances while guaranteeing no interference to protection schemes when no cyber attack is ongoing. Furthermore, it meets IEC 61850-5 and IEC 61869-9 strict latency requirements and required throughput, respectively. The method is robust to communication network latency variations and time synchronization issues. Thus, it provides a viable solution to enhance cyber security and resilience in digital substations. Although the method was validated on IEC 61850-compliant testbeds, future work consists in the further engineering of the proposed method and its testing in real digital substations. Moreover, advanced attacker techniques capable of maximizing the likelihood of malicious SV frames acceptance, and how to defend against such advanced threats, will be investigated.

REFERENCES

- [1] D. U. Case, "Analysis of the cyber attack on the ukrainian power grid," Electricity Information Sharing and Analysis Center (E-ISAC), Tech. Rep. 1-29, 2016.
- [2] J. Slowik, "Crashoverride: Reassessing the 2016 ukraine electric power event as a protection-focused attack," Dragos, Inc, Tech. Rep., 2019.
- [3] P. Kozak, I. Klaban, and T. Šlajs, "Industroyer cyber-attacks on Ukraine's critical infrastructure," in *2023 International Conference on Military Technologies (ICMT)*, May 2023, pp. 1–6. [Online]. Available: <https://ieeexplore.ieee.org/document/10171308>
- [4] C. Cimpanu, "Uk electricity middleman hit by cyber attack," 2024. [Online]. Available: <https://www.zdnet.com/article/uk-electricity-middleman-hit-by-cyber-attack/>
- [5] J. D. Christopher, "Sans 2024 ics/ot survey: The state of ics/ot cybersecurity," SANS Institute, Tech. Rep., Oct 9 2024.
- [6] V. S. Rajkumar, M. Tealane, A. Stefanov, A. Presekhal, and P. Palensky, "Cyber Attacks on Power System Automation and Protection and Impact Analysis," in *2020 IEEE PES Innovative Smart Grid Technologies Europe (ISGT-Europe)*. The Hague, Netherlands: IEEE, Oct. 2020, pp. 247–254. [Online]. Available: <https://ieeexplore.ieee.org/document/9248840/>
- [7] V. S. Rajkumar, A. Ştefanov, J. L. Rueda Torres, and P. Palensky, "Dynamical Analysis of Power System Cascading Failures Caused by Cyber Attacks," *IEEE Transactions on Industrial Informatics*, vol. 20, no. 6, pp. 8807–8817, Jun. 2024. [Online]. Available: <https://ieeexplore.ieee.org/document/10479971>
- [8] J. Gaspar, T. Cruz, C.-T. Lam, and P. Simões, "Smart Substation Communications and Cybersecurity: A Comprehensive Survey," *IEEE Communications Surveys & Tutorials*, vol. 25, no. 4, pp. 2456–2493, 2023. [Online]. Available: <https://ieeexplore.ieee.org/abstract/document/10217175>
- [9] H. Zhou, Y. Zheng, J. Xu, Y. Li, and J. Cao, "Propagation Delay Measurement and Evaluation for SV Based on HSR Networks," *IEEE Transactions on Industrial Informatics*, vol. 18, no. 6, pp. 3970–3977, Jun. 2022. [Online]. Available: <https://ieeexplore.ieee.org/document/9519509>
- [10] S. M. S. Hussain, M. A. Aftab, S. M. Farooq, I. Ali, T. S. Ustun, and C. Konstantinou, "An Effective Security Scheme for Attacks on Sample Value Messages in IEC 61850 Automated Substations," *IEEE Open Access Journal of Power and Energy*, vol. 10, pp. 304–315, 2023, conference Name: IEEE Open Access Journal of Power and Energy. [Online]. Available: <https://ieeexplore.ieee.org/document/10065529>
- [11] J. Hong, R. Karnati, C.-W. Ten, S. Lee, and S. Choi, "Implementation of Secure Sampled Value (SeSV) Messages in Substation Automation System," *IEEE Transactions on Power Delivery*, vol. 37, no. 1, pp. 405–414, Feb. 2022, conference Name: IEEE Transactions on Power Delivery. [Online]. Available: <https://ieeexplore.ieee.org/document/9361308>
- [12] M. F. Elrawy, C. Fioravanti, G. Oliva, M. K. Michael, and R. Setola, "A Geometrical Approach to Enhance Security Against Cyber Attacks in Digital Substations," *IEEE Access*, vol. 12, pp. 18724–18738, 2024, conference Name: IEEE Access. [Online]. Available: <https://ieeexplore.ieee.org/document/10418934>
- [13] M. Rodríguez, J. Lázaro, U. Bidarte, J. Jiménez, and A. Astarloa, "A Fixed-Latency Architecture to Secure GOOSE and Sampled Value Messages in Substation Systems," *IEEE Access*, vol. 9, pp. 51646–51658, 2021, conference Name: IEEE Access. [Online]. Available: <https://ieeexplore.ieee.org/document/9387365>
- [14] S. M. Suhail Hussain, "Lightweight Optimized Message Authentication Scheme for IEC 61850 Sampled Value Messages," *IEEE Transactions on Power Delivery*, vol. 39, no. 4, pp. 2552–2555, Aug. 2024. [Online]. Available: <https://ieeexplore.ieee.org/document/10521708>
- [15] T. S. Ustun, S. M. S. Hussain, L. Yavuz, and A. Onen, "Artificial Intelligence Based Intrusion Detection System for IEC 61850 Sampled Values Under Symmetric and Asymmetric Faults," *IEEE Access*, vol. 9, pp. 56486–56495, 2021, conference Name: IEEE Access. [Online]. Available: <https://ieeexplore.ieee.org/document/9395448>
- [16] J. Mo and H. Yang, "Sampled Value Attack Detection for Busbar Differential Protection Based on a Negative Selection Immune System," *Journal of Modern Power Systems and Clean Energy*, vol. 11, no. 2, pp. 421–433, 2023. [Online]. Available: <https://ieeexplore.ieee.org/document/9718131>
- [17] M. El Hariri, E. Harmon, T. Youssef, M. Saleh, H. Habib, and O. Mohammed, "The IEC 61850 Sampled Measured Values Protocol: Analysis, Threat Identification, and Feasibility of Using NN Forecasters to Detect Spoofed Packets," *Energies*, vol. 12, no. 19, p. 3731, Jan. 2019, number: 19 Publisher: Multidisciplinary Digital Publishing Institute. [Online]. Available: <https://www.mdpi.com/1996-1073/12/19/3731>
- [18] S. Hussain, S. M. S. Hussain, M. Hemmati, A. Iqbal, R. Alammari, S. Zanero, E. Ragaini, and G. Gruosso, "A novel hybrid cybersecurity scheme against false data injection attacks in automated power systems," *Protection and Control of Modern Power Systems*, vol. 8, no. 3, pp. 1–15, Jul. 2023, conference Name: Protection and Control of Modern Power Systems. [Online]. Available: <https://ieeexplore.ieee.org/document/10374446>
- [19] K. Wannous, P. Toman, V. Jurák, and V. Wasserbauer, "Analysis of IEC 61850-9-2LE Measured Values Using a Neural Network," *Energies*, vol. 12, no. 9, p. 1618, Jan. 2019, number: 9 Publisher: Multidisciplinary Digital Publishing Institute. [Online]. Available: <https://www.mdpi.com/1996-1073/12/9/1618>
- [20] J. Hong, C.-C. Liu, and M. Govindarasu, "Integrated Anomaly Detection for Cyber Security of the Substations," *IEEE Transactions on Smart Grid*, vol. 5, no. 4, pp. 1643–1653, Jul. 2014, conference Name: IEEE Transactions on Smart Grid. [Online]. Available: <https://ieeexplore.ieee.org/document/6786500>
- [21] —, "Detection of cyber intrusions using network-based multicast messages for substation automation," in *ISGT 2014*, Feb. 2014, pp. 1–5. [Online]. Available: <https://ieeexplore.ieee.org/abstract/document/6816375>
- [22] A. Eynawi, A. Mumrez, G. Elbez, and V. Hagenmeyer, "Machine Learning-Based Feature Selection for Intrusion Detection Systems in IEC 61850-Based Digital Substations," in *2024 IEEE International Conference on Communications, Control, and Computing Technologies for Smart Grids (SmartGridComm)*, 2024, p. 7. [Online]. Available: <https://publikationen.bibliothek.kit.edu/1000176614>
- [23] A. Delhomme, L. O. Nweke, and S. Y. Yayilgan, "Detecting denial of service attacks in smart grids using machine learning: A study of iec 61850 protocols," in *Proceedings of the Eighteenth International Conference on Emerging Security Information, Systems, and Technologies (SECURWARE 2024)*, Nice, France, 2024, pp. 1–6.
- [24] F. Manzoor, V. Khattar, C.-C. Liu, and M. Jin, "Zero-day Attack Detection in Digital Substations using In-Context Learning," in *2024 IEEE International Conference on Communications, Control, and Computing Technologies for Smart Grids (SmartGridComm)*, Sep. 2024, pp. 220–225, iSSN: 2474-2902. [Online]. Available: <https://ieeexplore.ieee.org/abstract/document/10738025>
- [25] J. Hong and C.-C. Liu, "Intelligent Electronic Devices With Collaborative Intrusion Detection Systems," *IEEE Transactions on Smart Grid*, vol. 10, no. 1, pp. 271–281, Jan. 2019. [Online]. Available: <https://ieeexplore.ieee.org/document/8006250>
- [26] N. Benvenuto and M. Zorzi, *Principles of communications Networks and Systems*. John Wiley & Sons, 2011.
- [27] S. Ali, J. Ara, and I. Shah, "A comparison of different parameter estimation methods for exponentially modified Gaussian distribution," *Afrika Matematika*, vol. 33, no. 2, p. 58, May 2022. [Online]. Available: <https://doi.org/10.1007/s13370-022-00995-w>
- [28] J. Olivier and M. M. Norberg, "Positively skewed data: revisiting the Box-Cox power transformation," *International Journal of Psychological Research*, vol. 3, no. 1, pp. 68–75, 2010.